Epitaxial Stabilization of Ferromagnetism in the Nanophase of FeGe

Changgan Zeng,[1] P. R. C. Kent,[2] M. Varela,[3] M. Eisenbach,[4] G. M. Stocks,[4]
Maria Torija,[1] Jian Shen,[3,1] and Hanno H. Weitering[1,3]

[1]*Department of Physics and Astronomy, The University of Tennessee, Knoxville, Tennessee 37996, USA*
[2]*Computer Science and Mathematics Division, Oak Ridge National Laboratory, Oak Ridge, Tennessee 37831, USA*
[3]*Condensed Matter Sciences Division, Oak Ridge National Laboratory, Oak Ridge, Tennessee 37831, USA*
[4]*Metals and Ceramics Division, Oak Ridge National Laboratory, Oak Ridge, Tennessee 37831, USA*

(Received 1 June 2005; published 28 March 2006)

Epitaxial nanocrystals of FeGe have been stabilized on Ge(111). The nanocrystals assume a quasi-one-dimensional shape as they grow exclusively along the $\langle 1\bar{1}0\rangle$ direction of the Ge(111) substrate, culminating in a compressed monoclinic modification of FeGe. Whereas monoclinic FeGe is antiferromagnetic in the bulk, the nanowires are surprisingly strong ferromagnets below ~200 K with an average magnetic moment of $0.8\mu_B$ per Fe atom. Density functional calculations indicate an unusual stabilization mechanism for the observed ferromagnetism: lattice compression destabilizes the antiferromagnetic Peierls-like ground state observed in the bulk while increased *p-d* hybridization suppresses the magnetic moments and stabilizes ferromagnetism.

DOI: 10.1103/PhysRevLett.96.127201 PACS numbers: 75.75.+a, 68.55.Ac, 75.50.Ee, 75.70.−i

Magnetism and structure are strongly intertwined [1,2], particularly in nanoscale systems [3,4]. As a rule of thumb, an increasing lattice constant enhances the magnetic moment and potentially stabilizes ferromagnetism. Both of these properties are highly desirable for applications. To increase the lattice constant of a low-dimensional or nanoscale structure, the most common approach is to epitaxially stabilize a magnetic thin film under tensile strain using a suitable substrate. Unfortunately, the allowable increase of the lattice parameter is limited by epitaxial strain relaxation and is rarely sufficient to form new magnetic phases. Interesting exceptions include epitaxially grown fcc Fe films on Cu, which exhibit a range of magnetic phases including antiferromagnetism, low-spin ferromagnetism, and high-spin ferromagnetism upon a small variation of the lattice constant [5].

In this Letter, we report on a novel nanophase material that is epitaxially compressed *and* ferromagnetic at the nanoscale ($T_c \sim 200$ K) while being antiferromagnetic in the bulk, namely, FeGe on Ge(111). Bulk FeGe exhibits a very interesting variety of structures and magnetic properties [6–8]. It crystallizes in three different polymorphs. The cubic polymorph is an antiferromagnetic metal with a Dzyaloshinskii-Moriya–type spin spiral [6], while the hexagonal [7] and monoclinic [8] polymorphs exhibit complex, modulated spin structures with a net antiferromagnetic magnetization. The FeGe nanocrystals, on the other hand, appear to be strongly ferromagnetic. Their shape gradually evolves as a function of annealing temperature, culminating in the formation of long nanowires that can be identified as a highly strained, yet perfectly coherent monoclinic polymorph of FeGe. Density functional calculations demonstrate that *compressive* strain, not tensile strain, tips the delicate balance of competing exchange interactions into a collective ferromagnetic response. These FeGe nanowires present a first example of *volume ferromagnetism* in nanophases of an antiferromagnetic compound. Many other examples likely exist. In particular, rare-earth silicides on silicon form very similar nanowires; their magnetic properties remain to be explored [9–11].

Ge(111) substrates were cleaned by cycles of Ne-ion sputtering and annealing. FeGe nanocrystals were produced by depositing Fe onto Ge(111) in ultrahigh vacuum at room temperature and subsequent annealing for about 10 min. The absolute Fe coverage was determined with Rutherford backscattering spectrometry [12].

The evolution of the surface morphology was studied as a function of annealing temperature between 0.3 to 2.0 monolayer (ML) of Fe. Figure 1(a) shows a scanning tunneling microscopy (STM) image of the surface morphology after deposition of 2 ML of Fe on Ge(111). The Fe

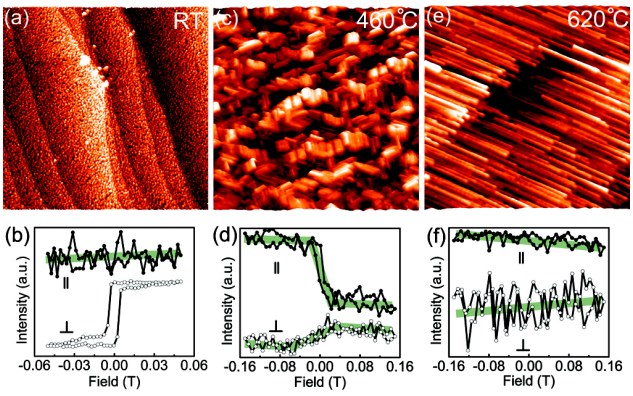

FIG. 1 (color online). STM images (500 nm × 500 nm) (top) and corresponding MOKE data (bottom) of Fe and Fe-Ge nanocrystals on Ge(111). The Fe coverage is 2 ML, and MOKE data were recorded at 77 K. Annealing temperatures and magnetic field orientations (∥ , ⊥) are indicated.

 © 2006 The American Physical Society

atoms aggregate into small clusters. Magneto-optical Kerr effect (MOKE) measurements in Fig. 1(b) reveal a ferromagnetic hysteresis loop with an easy axis of magnetization that is perpendicular to the film. Crystallites with a well-defined, elongated shape form after annealing to 460 °C, as is shown in Fig. 1(c). These alloy crystallites are also ferromagnetic, but their Kerr response is weaker and the easy axis of magnetization has changed to *in plane* [Fig. 1(d)]. Still higher annealing temperatures lead to longer nanocrystals and vanishing Kerr response. Figure 1(e) shows the morphology after annealing to 620 °C. The surface is covered with long "nanowires" that are aligned along the three equivalent $\langle 1\bar{1}0\rangle$ directions of the Ge substrate. They average 165 nm in length, 6 nm in width, and 1.0 nm in height. This remarkable unidirectional growth of the nanocrystals indicates one-dimensional lattice matching along the Ge$\langle 1\bar{1}0\rangle$ direction (which has a repeat distance of 4.0 Å), analogous to the nanowire growth of rare-earth silicides on Si [9–11].

At a reduced coverage of 0.3 ML, it is possible to obtain atomic resolution from the exposed Ge(111)-$c(2\times 8)$ substrate (not shown), and near-atomic resolution from the nanowires [Fig. 2(a)]. From the latter, we obtain the approximate unit cell dimensions (4.0 ± 0.5) Å $\times$ (11.5 ± 0.5) Å, which matches the unit cell parameters in the (a, b) plane of monoclinic FeGe ($a = 11.84$ Å, $b = 3.94$ Å, $c = 4.94$ Å, and $\beta = 103.51°$) [8].

In order to definitively identify the structure and composition of this novel nanophase, we capped the sample with a thin amorphous Si layer for *ex situ* scanning transmission electron microscopy (STEM) and electron energy loss spectroscopy (EELS), using a VG HB501 UX microscope. Cross-sectional specimens for STEM were prepared by grinding, dimpling, and Ar ion milling. Because the thinnest wires did not survive sample processing, we show the STEM images of some thicker wires from a sample with a nominal coverage of 2 ML.

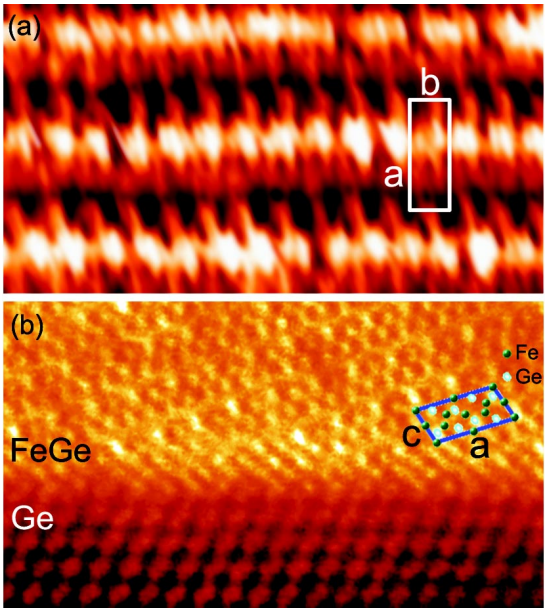

FIG. 2 (color online). (a) Nearly atomic-resolved STM images of a monoclinic FeGe nanocrystal, after annealing to 700 °C, with V_s of 1.0 V. The nominal coverage is 0.3 ML. (b) Z-contrast high-resolution image of the interface between the FeGe nanowire and the Ge substrate. The monoclinic unit cell has been highlighted. The coverage is 2.0 ML.

Figure 2(b) shows an atomic-resolution Z-contrast cross-sectional image of a FeGe nanowire on the Ge(111) substrate. The crystal structure is definitely monoclinic [8], and the interface appears perfectly coherent and free of defects. In this projection, the substrate is oriented with the [110] zone axis, while the wire has the [010] direction pointing out of the plane. The a axis lies almost parallel to the interface, with a mistilt of about 16°, as shown in Fig. 2(b). From the analysis of the images, the lattice constants were measured to be $a = 10.5 \pm 0.1$ Å, $c = 5.0 \pm 0.1$ Å, and $\beta = 103.7° \pm 0.2°$, thus showing very significant amounts of epitaxial strain. The monoclinic b axis is parallel to the wire direction and matches the Ge$\langle 1\bar{1}0\rangle$ direction, i.e., $b = 4.0$ Å. Routine EELS analysis using the Fe L edge at 708 eV and the Ge L edge at 1217 eV shows that the stoichiometry of the wire corresponds to a Fe:Ge ratio of 1:1 with error bar about 10%, or equivalently $Fe_{0.5\mp x}Ge_{0.5\mp x}$, $x < \sim 0.05$. The end phase of the annealing series is therefore conclusively identified as monoclinic FeGe.

The morphological evolution of the nanocrystals upon annealing is accompanied by the initial reorientation of the magnetization and gradual reduction of the Kerr response (Fig. 1). To further investigate the origin of the reduced Kerr response, we performed *ex situ* SQUID measurements on capped and uncapped samples with a total Fe coverage of 2.0 ML. SQUID results are identical for both samples, showing that the FeGe nanocrystals are stable against capping and oxidation. Interestingly, the ferromagnetic saturation moment from SQUID measured at 5 K depends on the annealing temperature and evolution stage of the nanocrystals. For instance, the magnetic moment per Fe atom at 5 K is $1.5 \pm 0.2\mu_B$ when the Fe deposit is annealed at 460 °C, $0.9 \pm 0.2\mu_B$ when annealed at 620 °C, and $0.8 \pm 0.2\mu_B$ when annealed at 700 °C. Surprisingly, the monoclinic nanowires are ferromagnetic (Fig. 3), even though the monoclinic bulk phase is antiferromagnetic [8]. The inset of Fig. 3 shows ferromagnetic hysteresis loops of the monoclinic nanocrystals. The average saturation moment per Fe atom is $0.8\mu_B$ at 5 K. Figure 3 also shows the magnetization as a function of temperature. Remanence vanishes near 200 K, while the field-induced moment disappears near 250 K. The gradual disappearance of the MOKE signal upon annealing (Fig. 1) is attributed to the reduction of the ferromagnetic moment (as measured by SQUID), combined with the reduced intensity of the reflected laser beam with the changing surface morphology. Eventually, the signal-to-noise ratio of the Kerr intensity dropped below the detection limit of the MOKE setup.

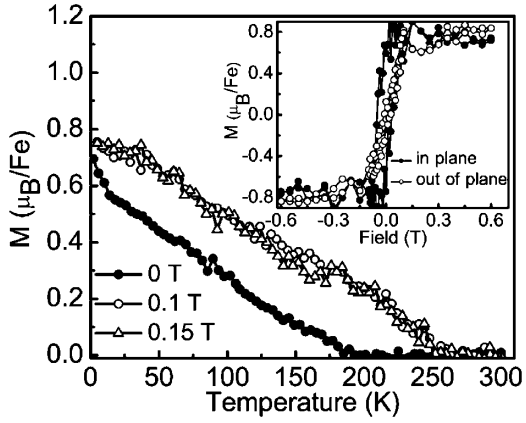

FIG. 3. Remanent and field-induced magnetization of monoclinic FeGe nanowires, formed at 700 °C, as a function of temperature for in-plane magnetic field. The inset shows the field-dependent magnetization at $T = 5$ K for in-plane and out-of-plane magnetic field, showing clear evidence of ferromagnetism.

Ferromagnetism in nanoparticles of antiferromagnetic materials is usually attributed to uncompensated spins at the surface or interface of the nanoparticle, as originally proposed by Néel [13]. Alternatively, Mørup and Fransdsen [14] recently argued that magnetic sublattices in antiferromagnetic nanostructures precess in such a way that the moments are not exactly antiparallel, resulting in a net magnetization that *increases* with temperature. Either way, the net magnetization is expected to be very small. For instance, NiO and CoO nanoparticle systems have spontaneous moments that are smaller than $0.1\mu_B$ per magnetic atom [15,16]. Ferromagnetism in FeGe nanowires, on the other hand, amounts to $\sim 1\mu_B$ per Fe and must be a true *volume* phenomenon.

Ferromagnetism in monoclinic FeGe nanowires may be explained on the basis of the peculiar electronic structure of bulk FeGe and related compounds, where the electronic structure and magnetic properties appear to be strongly sensitive to the lattice constant [17–19]. To establish the possible role of epitaxial strain in stabilizing ferromagnetism in monoclinic FeGe, we performed *ab initio* projector-augmented wave (PAW) density functional calculations [20] for the 16 atom unit cell monoclinic structure. For bulk calculations we utilized a well-converged 25 Ry plane-wave cutoff and $4 \times 8 \times 8$ Monkhorst-Pack k-point grid for tetrahedral Brillouin zone integration. Lattice vectors were relaxed until the external pressure was 1 kbar or less. To establish the lowest energy antiferromagnetic ground state, we performed a combinatorial search over all 1680 potential magnetic configurations. For the relaxed bulk monoclinic structure we find a delicate balance between ferromagnetism and antiferromagnetism: within the generalized gradient approximation (GGA) [21] antiferromagnetism is favored by 0.016 eV/cell, while in the local density approximation [22] ferromagnetism is favored by 0.091 eV/cell. GGA calculations using a larger $6 \times 12 \times 12$ k-point grid again favor antiferromagnetism by 0.015 eV/cell. The average calculated moment of the ferromagnetic phase is $1.41\mu_B$ per Fe atom, with individual moments $0.96(\times 2)$, $1.5(\times 2)$, and $1.8(\times 4)\mu_B$. The primitive cell of monoclinic FeGe has four a-b planes of Fe atoms stacked along the c axis; in the lowest energy antiferromagnetic configuration these planes are individually antiferromagnetic.

Experimentally, the overall antiferromagnetic structure of the monoclinic phase is complex [8]. It is clear, however, that the bulk magnetic structure or spin density exhibits an incommensurate modulation along the monoclinic b axis, so that the a-c planes appear ferromagnetic. Our calculated magnetic structure is similar to the structure proposed from neutron diffraction [8], but we do not reproduce the complex spin structure on the Fe a sites [8] due to the exclusion of noncollinear magnetism and spin spirals from our calculations.

We surveyed the electronic structure as a function of epitaxial conditions, varying the a and b lattice vectors, while fully relaxing all atomic positions and c axis for both ferromagnetic and antiferromagnetic states. For efficiency we fixed the monoclinic angle $\beta = 103.5°$ and used a $2 \times 2 \times 4$ k-point grid. In Fig. 4 we show the calculated difference in antiferromagnetic and ferromagnetic total energies as a function of the in-plane lattice constants. The contours and lowest energy configurations were obtained from a 20×6 grid of calculations in the a-b plane. The data show that the magnetic ground state of FeGe depends sensitively on the lattice constants: compression along the a axis and expansion along the b axis favors ferromagnetism; at the experimentally identified lattice constants ($a = 10.5 \pm 0.1$ Å, $b = 4.0$ Å, Fig. 2), ferromagnetism is strongly favored. The calculated c lattice parameter is 5.1 Å, in excellent agreement with the measured 5.0 ± 0.1 Å. The average magnetic moment is $1.37\mu_B$. Examination of the full a-, b-, and c-axis dependence of both ferromagnetic and antiferromagnetic energies found no evidence for stable structures at lattice parameters other than the bulk.

The largest contribution to stabilizing ferromagnetism is due to *compression* along the a axis. This counterintuitive result has the opposite sense to MnSi [23], where pressure drives antiferromagnetism, underscoring the complex bal-

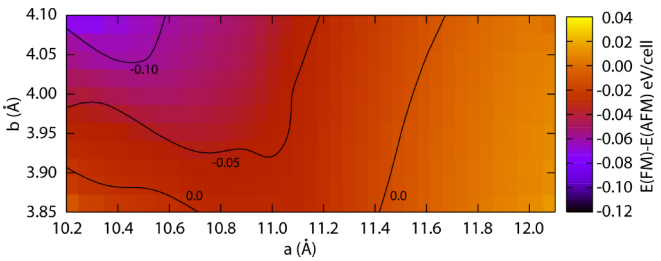

FIG. 4 (color online). Calculated energy differences between ferromagnetic (FM) and antiferromagnetic (AFM) ground states of monoclinic FeGe. Approximate energy contours are shown.

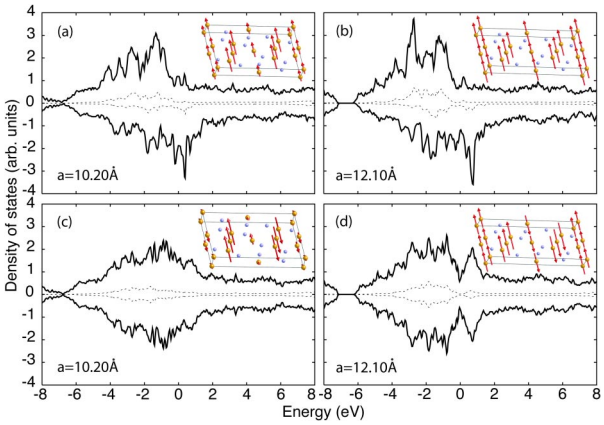

FIG. 5 (color online). Density of states of (a),(b) ferromagnetic and (c),(d) antiferromagnetic FeGe, calculated for (a),(c) $a = 10.2$ Å and (b),(d) $a = 12.1$ Å, using PAW density functional theory and the GGA. Dashed lines show the projected Fe $3d$ component. Insets are visualizations of the resultant spin structures. The Fe d moments are indicated by the length and orientation of each arrow. The Fermi energies are aligned at 0 eV. A 50 meV Gaussian broadening was applied.

ance of p-d hybridization and d-d interactions in the more complex FeGe. In order to understand how lattice compression can stabilize ferromagnetism, we examined the electronic structure for two extreme cases: $a = 10.2$ Å and $a = 12.1$ Å, corresponding to strong ferromagnetism and antiferromagnetism, respectively. In Fig. 5 we show the calculated density of states and magnetic moments. At both extremes, the ferromagnetic density of states and moments are broadly similar [Figs. 5(a) and 5(b)], while the antiferromagnetic structure is strongly dependent on a. At large a[Fig. 5(d)], a strong Fe $3d$-character peak develops above the Fermi energy (E_F); the existing $3d$ character below E_F is also enhanced, while the $3d$ character is depleted from the region around E_F. This indicates that a Peierls-like mechanism is responsible for the stabilization of antiferromagnetism in the bulk. However, at small a, increased hybridization suppresses the Fe moments, allowing ferromagnetism to dominate.

In conclusion, FeGe has been stabilized on Ge(111) in the form of strained monoclinic nanowires. These nanowires represent the first known example of volume ferromagnetism in the nanophase of an antiferromagnetic compound. Contrary to expectations, ferromagnetism is stabilized via epitaxial compression, which preempts the formation of the Peierls-like antiferromagnetic state observed in the bulk. These findings show that the complexity of competing interactions in some bulk materials can lead to surprising and potentially useful properties in the nanophase.

We thank L. C. Feldman for the RBS coverage calibration. This work is funded by NSF under Contract No. DMR 0306239 (FRG). This research used computational resources of the Center for Computational Sciences and was sponsored by the Offices of Basic Energy Sciences and Advanced Scientific Computing Research, U.S. Department of Energy. Oak Ridge National Laboratory is managed by UT-Battelle, LLC, for the U.S. Department of Energy under Contract No. DE-AC05-00OR22725.

[1] G. Ju *et al.*, Phys. Rev. Lett. **93**, 197403 (2004).
[2] S. Yuasa *et al.*, J. Phys. Soc. Jpn. **64**, 4906 (1995).
[3] J. Shen and J. Kirschner, Surf. Sci. **500**, 300 (2002).
[4] S. D. Bader, Surf. Sci. **500**, 172 (2002).
[5] J. Giergiel *et al.*, Phys. Rev. B **52**, 8528 (1995); R. D. Ellerbrock *et al.*, Phys. Rev. Lett. **74**, 3053 (1995); M. Straub *et al.*, Phys. Rev. Lett. **77**, 743 (1996); T. Asada and S. Blugel, Phys. Rev. Lett. **79**, 507 (1997); A. Biedermann *et al.*, Phys. Rev. Lett. **86**, 464 (2001); D. Qian *et al.*, Phys. Rev. Lett. **87**, 227204 (2001); A. Enders *et al.*, Phys. Rev. Lett. **90**, 217203 (2003).
[6] B. Lebech *et al.*, J. Phys. Condens. Matter **1**, 6105 (1989).
[7] J. Bernhard *et al.*, J. Phys. F **14**, 2379 (1984).
[8] G. P. Felcher *et al.*, J. Phys. C **16**, 6281 (1983), and references therein.
[9] Y. Chen, D. A. A. Ohlberg, and R. S. Williams, J. Appl. Phys. **91**, 3213 (2002).
[10] J. Nogami, B. Z. Liu, M. V. Katkov, C. Ohbuchi, and N. O. Birge, Phys. Rev. B **63**, 233305 (2001).
[11] Z. He, D. J. Smith, and P. A. Bennett, Appl. Phys. Lett. **86**, 143110 (2005).
[12] In our definition, 1 ML corresponds to the atomic density in the (110) plane of bcc Fe.
[13] L. Néel, in *Low Temperature Physics*, edited by C. Dewitt, B. Dreyfus, and P. D. de Gennes (Gordon and Beach, New York, 1962), p. 413.
[14] S. Mørup and C. Frandsen, Phys. Rev. Lett. **92**, 217201 (2004).
[15] S. A. Makhlouf *et al.*, J. Appl. Phys. **81**, 5561 (1997); R. H. Kodama *et al.*, Phys. Rev. Lett. **79**, 1393 (1997).
[16] Y. J. Tang *et al.*, Phys. Rev. B **67**, 054408 (2003).
[17] V. I. Anisimov *et al.*, Phys. Rev. Lett. **89**, 257203 (2002).
[18] S. Yeo *et al.*, Phys. Rev. Lett. **91**, 046401 (2003).
[19] H. Yamada *et al.*, Physica (Amsterdam) **329B–333B**, 1131 (2003).
[20] G. Kresse and D. Joubert, Phys. Rev. B **59**, 1758 (1999); G. Kresse and J. Hafner, *ibid.* **47**, R558 (1993); **49**, 14 251 (1994).
[21] J. P. Perdew *et al.*, Phys. Rev. B **46**, 6671 (1992).
[22] J. P. Perdew and A. Zunger, Phys. Rev. B **23**, 5048 (1981).
[23] C. Pfleiderer *et al.*, Nature (London) **414**, 427 (2001).